Pakistan Journal of Hydrocarbon Research
Vol. 17, (June 2007),p.95-102, 15 Figs. 1 Table.

Porosity Prediction using 3D Seismic Inversion Kadanwari Gas Field, Pakistan

Nasir Ahmad[1], Giacomo Spadini[2], Arshad Palekar[1], M. Asim Subhani[1]

ABSTRACT

In the western part of the Kadanwari field a gas-bearing stratigraphic trap was identified in the G-sand of Lower Goru formation by drilling the X well. However, due to poor reservoir properties the well was not commercial. Thus, the challenge was to locate and quantitatively evaluate a drilling target in the sand body, which would have porosity values beyond the known producible threshold in the area. With this aim, 250 km^2 of 3D seismic data was acquired in the area. The data was processed to pre-stack time migration, and acoustic impedance inversion was performed. This inverted data was used to generate a pseudo porosity volume to locate a "sweet spot" for porosity in the area. A linear relationship between Porosity and Acoustic Impedance was built based on the wire-line and CPI logs of the well X. The equation was obtained as a regression line for the clean G-sand porosity and acoustic impedance. The equation was applied to the available AIMP volume to obtain a pseudo-porosity volume. The inversion-derived pseudo-porosity was compared with the CPI porosity at well X. As expected, the pseudo-porosity obtained from inversion provided a result with frequency content similar to the seismic data. For this reason the calculated porosity was not able to describe the details of internal variations of the G-Sand but capable to catch the bulk character of the target sand only. Using this pseudo-porosity volume, a pseudo-porosity map was generated. On the basis of this work, the successful well Y was drilled. Due to the presence of complex mineralogy the effective porosity of well Y is still a question, however the sonic porosity was very close to the predicted porosity of 17-18%. On the basis of this success the Kadanwari Joint Venture has decided to acquire 3D seismic in the all field area, to apply the same technique in order to fully evaluate the remaining potential. According to author's knowledge this technique has not been used previously in the area for porosity prediction.

INTRODUCTION

The Middle Indus Basin is a prolific basin located in the central part of Pakistan. The Kadanwari Gas Field is located in this gas prone basin (Figure 1). The field was discovered in 1989 and brought on stream in May 1995. In the original 1992 Field Development Plan the core area, which is the eastern part of the field was considered more prospective with E-sand of the Lower Goru as the reservoir (Nasir and Siddique, 2002). In Figure 1 the western part of the field, although structure was identified in early days, but was downgraded because it was below the known gas water contact (GWC) 3284mss, and distal (on E-sand level) compared to the eastern part. After initial years of production from different blocks it was established that the field has different compartments and each compartment may have its own GWC.

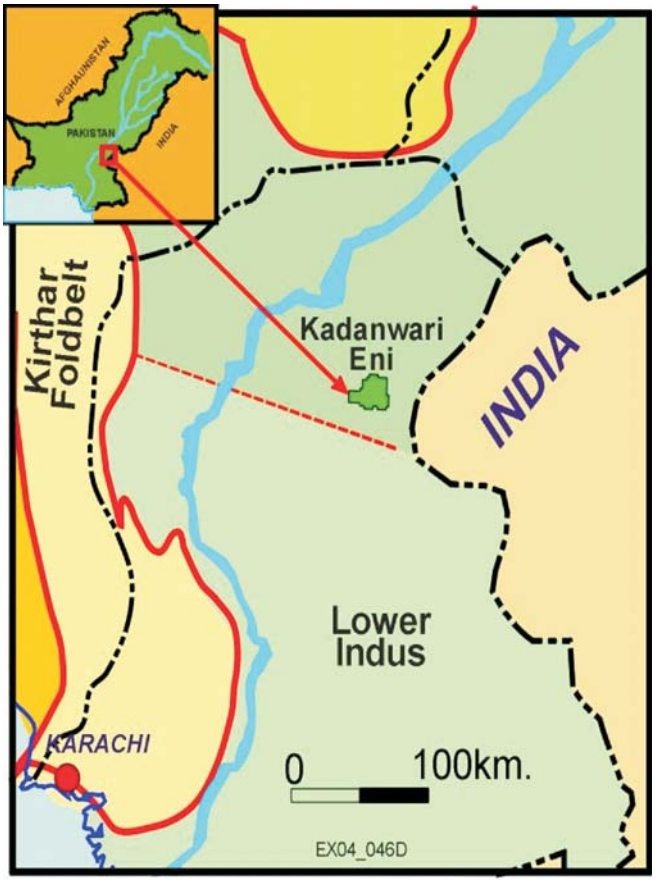

Figure 1- Location map of project area

In addition to it, the information of other wells in the adjacent area and successful testing the F-sand in 1999 of Lower Goru in K-7 and K-9 proved that shallower sands are also prospective(Nasir et al., 2002). This made the western part of the field more interesting. To test the potential of the structure in the western part of the field, the well X was drilled in 2001 with G-sand (younger than E-sand) of Lower Goru as the primary target (Figure 2). Although this well was not a commercial discovery due to poor reservoir quality sands, it proved the presence of gas bearing sand. The challenge was

[1] Eni Pakistan, 5th Floor, The Forum, G-20, Block 9, Khayaban-e-Jami, Clifton, 75600, Karachi, Pakistan
[2] Eni Petroleum, Suite # 3500, 1201 Louisiana Street, Houston, TX 77002, USA

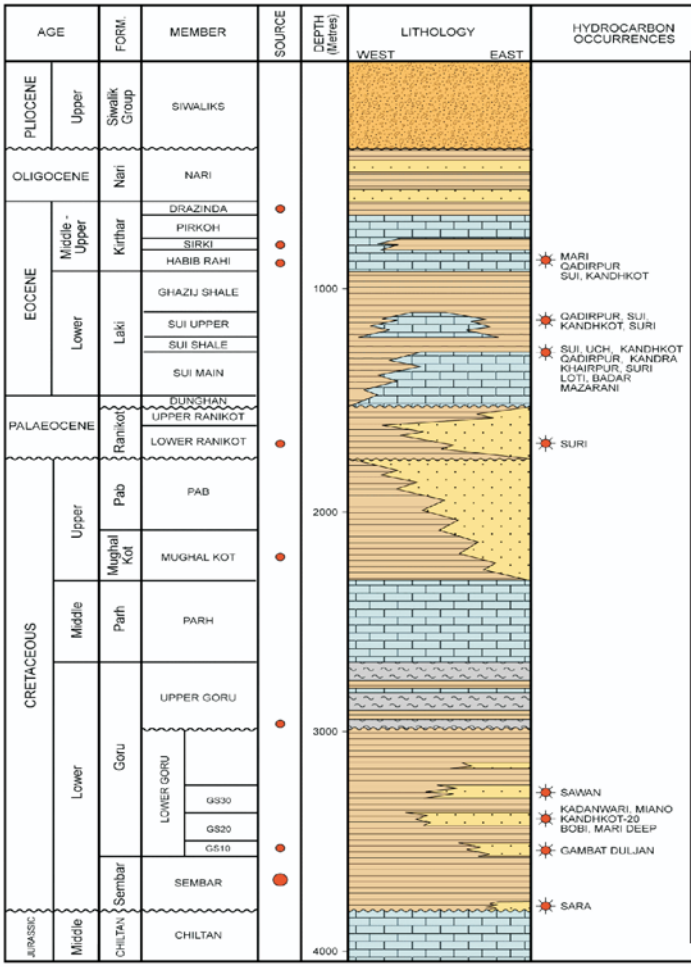

Figure 2- Generalized Stratigraphic Column of Middle Indus Basin

to locate a good porosity zone in this sand body and for this reason a 250 km^2 of 3D seismic data was acquired in this area. The data was processed to pre-stack time migration, and then acoustic impedance inversion was done. This inverted data was used to generate pseudo porosity volume to locate the good porosity zones in the area.

In order to establish the relation between porosity and acoustic impedance, the data of well 'X' were used. On the basis of this work along with other geological studies the well 'Y' was located, that successfully tested gas at a rate of 15mmscfd. In this manner, the proposed technique was proved successful to locate better porosity zones in the area, which is a major issue in the lower Goru sands of Middle Indus Basin. Authors suggest that this method can be applied for other areas, however, the careful data processing by preserving the relative amplitude is the key to success.

GEOLOGY & LOCAL STRATIGRAPHY

Kadanwari field is located on the SE flank of the Jacobabad High in the Middle Indus Basin . In east of Kadanwari some gas fields are also present in India.

Three tectonic events are responsible for the structural configuration of the field. First is Late Cretaceous uplift and erosion, the axis of uplift appears to be oriented NNE-SSW but the degree of the uplift is uncertain. The second is right-lateral wrench faults, which are basement rooted. These have a general NNW-SSE orientation and exhibit 'flower structure' cross section profiles. The third event is Late Tertiary to recent uplift/inversion of the Jacobabad High having a major influence on the Kadanwari, and is responsible for stratigraphic and structural traps in the area.

The Lower Goru has layers of sand and shale. These sands act as reservoir rock with rapidly varying reservoir characteristics within a few km. In gross terms, these sands represent a shoreline estuarine system subject to both long shore currents and tidal influence. The major influence on these two processes was the degree of sand supply.

The Lower Goru sands has been divided into further sub units of Sand. Each company working in the area has its own subdivision, here we are following the LASMO subdivision which has divided reservoir units into seven sand bearing members, B to H. The main producing sands in the area are E and G but D, and F have also produced in few wells. The source of the Lower Goru sands is considered to be the Indian Shield to the south and east, locally prograding or aggrading sands are deposited during an overall rise in sea level; the resultant “backstepping” of successive reservoir units provides the conditions for marine flushing of a regressive sand pod during an overlying transgressive marine episode. The depositional strike of the shoreline sands is assumed to be approximately north-south to northeast-southwest. Reservoir quality in the productive E and G sands is good for a reservoir at 3300m depth, with porosity averaging 18-21% and permeability up to Darcies. Petrographic analysis suggests that this preservation of porosity and lack of cementation is probably due to the presence of early diagenetic, grain coating, chloritic clays, which inhibited cement growth. However, a moderately high level of this early authigenic chlorite decreases the reservoir quality by occluding the pores, which results in increase microporosity at the expense of macroporosity and elevated water saturation.

In the study area the main producer is G-sand which is about 60m thick and within the limit of seismic resolution. However internal prograde geometry is further improved by inversion.

SEISMIC DATA ACQUISITION

A total of 250 sq km of 3D land seismic data was recorded in western part of the Kadanwari Field for Tajjal JV between July and October in 2002. The objective of the 3D survey was to improve imaging of the structural and stratigraphic definition of the sand-bearing members G and E of the Lower Goru, within the zone 2.0 to 2.5 Sec two way time, corresponding to a depth of 3000-3500m. In addition to this, the important objectives of the 3D seismic data acquisition were to follow the continuity of the main prograding sand body from the adjacent area, to use the seismic attributes to predict reservoir quality, and to perform seismic inversion to predict reservoir porosity. The survey area is characterized by sand dunes elongated NE-SW in the eastern part and by cultivated

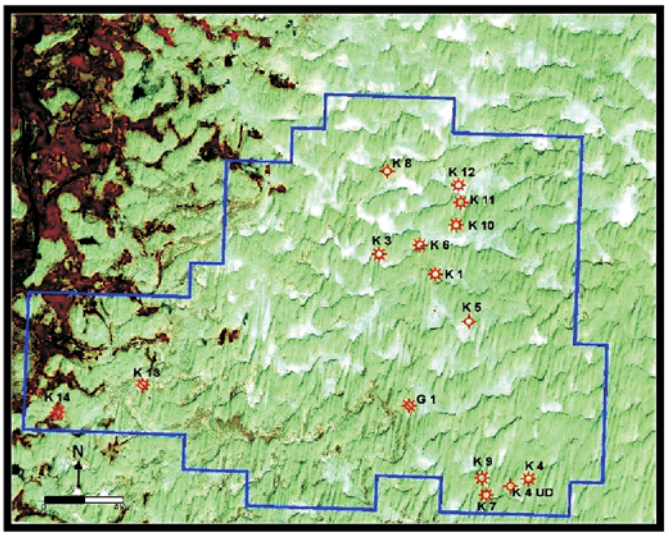

Figure 3- Satellite Imagery of Kadanwari

areas in the western part. The dunes reach 50m height in the southern part of the survey and have the southern slope that is steeper than the northern one (Figure 3). The survey was acquired using a cross-array technique. The receiver lines were SW-NE oriented (45º azimuth), and the shot lines were oriented SE-NW (315º azimuth). The survey had a total of 68 receiver lines with 17,208 receivers and 76 shot lines with 15,734 shots. Receiver and shot line spacing was 300m, and receiver and shot intervals were both 50m, producing a 25m x 25m CDP bin with nominal fold of 48. The survey consisted of 16 separate swaths, with 8 receiver lines and 144 live channels per receiver line for each shot.

The survey was acquired with mixed source, vibroseis and dynamite, with predominantly vibroseis to the southeast and dynamite in the cultivated areas in the northwest. The vibroseis parameters were 8 sweeps of 4 vibrators with a linear sweep of 8-80Hz for 12 seconds. For the dynamite source a single hole of nominally 21m was used with a charge of 4Kg.

SEISMIC DATA PROCESSING

The Kadanwari 3D volume was processed to Pre-Stack Time Migration (PSTM). A comprehensive series of processing parameter trials were conducted on selected shot records and panels of data with many processes being evaluated from whole in-line and cross-line stacks.

In the acoustic impedance inversion the basic assumption is that the amplitude is proportional to the reflectivity. This requires that the amplitude has been preserved faithfully and that there is no serious noise contributing to the amplitude(Pendrel and Van Riel, 1997). A major effort was directed at the preservation of relative amplitudes, with multiples passes of automatic trace and noise burst editing being required to clean the data sufficiently prior to running the PSTM and DMO, to avoid the introduction of undesirable artifacts. Relative amplitude stacks for each of the 786 in-lines were individually examined as a final QC, with any significant noise burst still present on the stack trace being individually edited from the CDP gather. Considerable time was also spent during the early stages of processing in analyzing and attempting to reduce the impact of the high amplitude noise cone. Effective matching of phase and amplitude of the vibroseis and dynamite sources was also an important factor in the quality of the final data. Special attention was paid to the following processes for relative amplitude preservation.

Gain Recovery

A series of trials were carried out on typical raw vibroseis and dynamite shot records. There was little to choose between the spherical divergence based on TV^2 and a T^2 gain. The records were well balanced in time, but most of the energy was concentrated in the near traces, with a high amplitude cone particularly on the vibroseis shots. It was decided to use the T^2 amplitude gain recovery for the early stages of processing, as this could be easily removed at a later stage and replaced with a TV^2 gain once more accurate velocities had been determined. The gain curve was held constant below 5.0 Secs. (Figures 4 and 5).

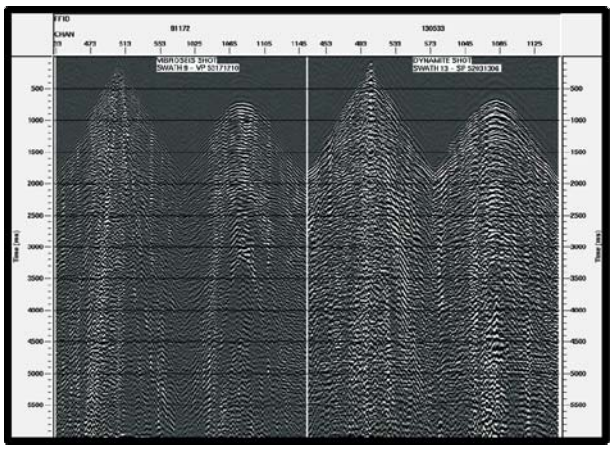

Figure 4- Near and offset raw vibroseis and dynnamite shots

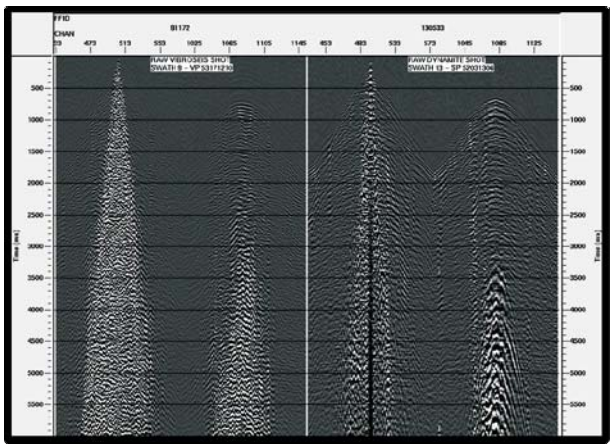

Figure 5- Near and offset raw shots with T2 amplitude recovery

Source Amplitude Balance

The overall amplitude level of the raw data differs greatly between the dynamite and vibroseis sources (Figure 4). In order to preserve relative amplitudes during the processing of the data it was necessary to match the overall amplitude level of the two sources. In order to compare the relative amplitudes of the two sources, all vibroseis and dynamite traces for a swath were analyzed separately with the high energy cone omitted from both sources. Based on this analysis a scale factor of 9.018 E-09 was selected and applied to the vibroseis data to match the overall level of the dynamite data.

Noise Cone Energy Balance

A high energy cone was seen on the vibroseis data having the full bandwidth, which would totally dominate a relative amplitude stack. The energy cone is weaker on the dynamite shots as these are located 21m deep, so surface noise is reduced (Figure 5). In order to preserve relative amplitude during processing there were two options available.

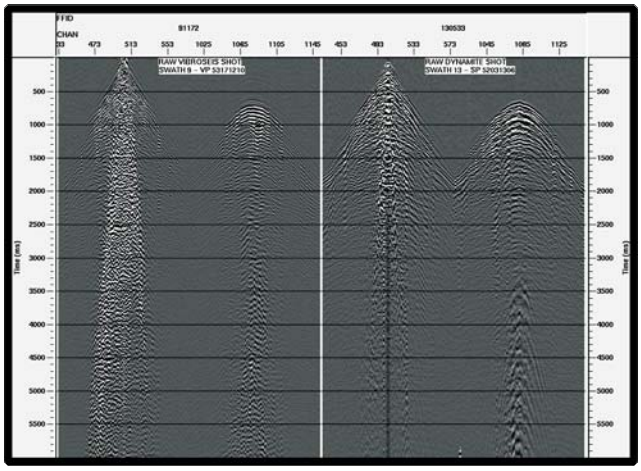

Figure 6- Near and far offset shot records with T2 amplitude recovery and low cut filter of 8 Hz 24dB/oct slope and noise cone balance of vibroseis and dynamite.

1) The high energy cone is removed by muting, so near offset information will be lost.

2) The amplitude level within the cone is reduced to match the data outside the cone, in the same way that the overall amplitudes of the two source types were analysed and matched (Figure 6). The overall amplitudes inside and outside reduce the energy level within the cone. There were some complications in that as the boundaries of the cone are not always well defined. The cone also contains some different amplitude bands within it, which are variable from shot to shot and different receiver lines within the same shot. The only feasible way of defining the cone was by absolute offset. There was little evidence of any useful reflection energy within the noise cone. This was demonstrated on relative amplitude and equalized test stacks with and without the noise cone muted out. Muting out the noise cone did not harm the stack, and actually improved continuity at depth. On this basis the decision was taken to mute out the noise cone.

Surface Consistent Amplitude Corrections

Shot and receiver amplitude corrections were computed excluding the noise cone from the analysis. The average amplitude of each trace was calculated and partitioned into source and receiver terms. An offset component was also calculated from the amplitude analysis, which can be applied to the data prior to stack, so that near and far traces have equal contribution to the stack if no offset term was applied during the initial gain recovery, as in the case of the simple T^2.

SEISMIC INVERSION

Wavelet analysis was conducted by computing a filter that best shaped the well log reflection coefficients to the input seismic at the well location. The phase of the seismic data, which may vary with frequency, was found from this filter. A constrained sparse spike inversion (CSSI) algorithm (Debeye and Van Riel, 1990) was chosen because it performs a deterministic seismic trace inversion to model the subsurface reflectivity. The algorithm minimized the misfit between the seismic data and synthetic seismograms. The algorithm was run iteratively, adjusting the amplitude and phase spectrum of the wavelet. The CSSI algorithm generates acoustic impedance results with a broader bandwidth than the seismic data. This algorithm minimizes the sum of the absolute values of the differences between data and the model. A key parameter of the algorithm is the factor which controls the trade off between the scarcity of the reflectivity series and fit of the generated acoustic impedance to the seismic data. Well data is used in the inversion to constrain results to remain within a fairway of values defined by the well acoustic impedance log. The acoustic impedance volume is further evaluated to predict the porosity. The inverted acoustic impedance volume was highlighting the acoustic properties of layers rather than of the interfaces, and clearly demonstrated the improved interpretability of the prograding bodies of the G-sand reservoir. In particular it was now possible to resolve the presence of two different prograding units of the G-sand. Furthermore, the top and the bottom of the reservoir could now be better defined and a more detailed estimate of the thickness of the net sand be obtained.

POROSITY PREDICTION

Once obtaining an acoustic impedance volume it was possible to generate a pseudo porosity volume for porosity prediction in the area. In order to do porosity prediction a pseudo porosity volume was generated and the following steps were taken.

1. A linear relationship between porosity and acoustic impedance was built based on the wire-line and CPI logs from existing well X. From this plot the following equation was derived: $\varphi = m(AIMP)+c$

Where φ is the porosity, m is the slope, AIMP is the acoustic

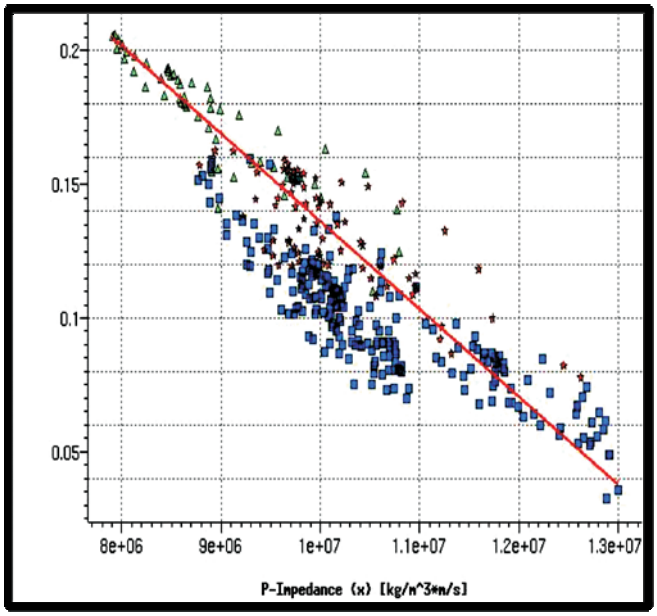

Figure 7- Cross-plots of effective porosity versus acoustic impedance between to G porosity and G porosity markers of well X showing the porosity regression line in red.

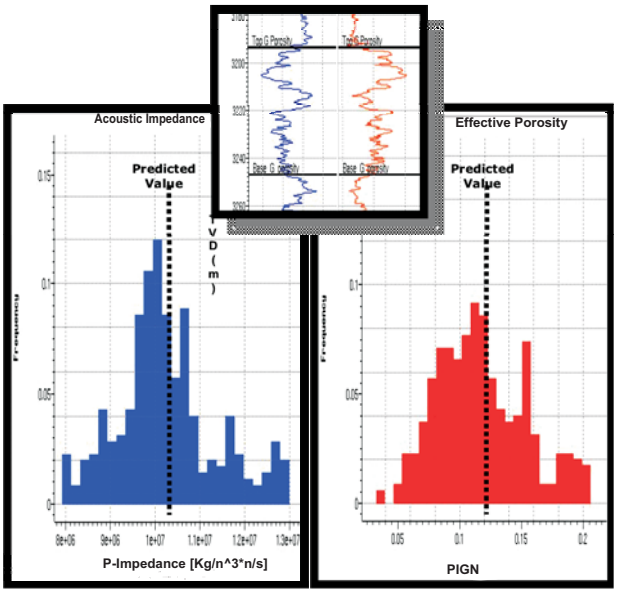

Mean Acoustic Impedance (log data) : 1.014e+7
Max AIMP Predicted : 1.030e+7

Mean Effective Porosity (log data) : 0.1171
Max. Porosity Predicted : 0.122

Figure 9- Calibration to real data of well X over the Top-G porosity of Base-G Porosity

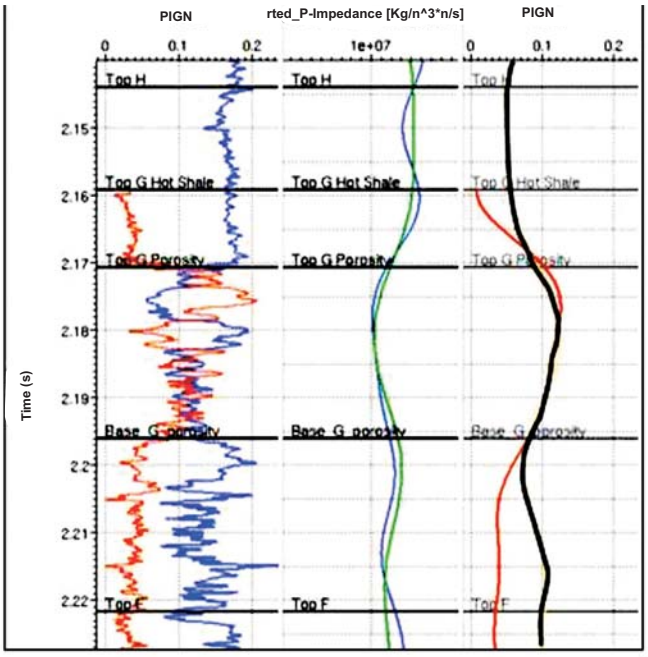

Figure 8- Well X logs displwr: effectove prpsotu (red) and acpostoc impedamce (blue) logs (1st panel); band-pass (0-0.50); Hz acoustic impedance log (green) trace (2nd panel); calculated porosity from inverted acoustic impedance (black) and band-pass (0.05) Hz porosity log (red) trace (3rd panel)

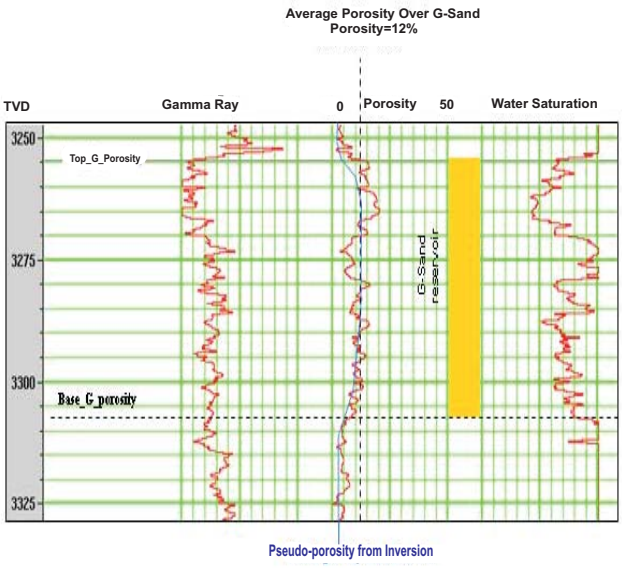

Figure 10- Well X Logs and pseudo porosity inversion at well X location

impedance and c is the intercept. The equation was obtained as a regression line for the clean G-sand (VCL < 0.2) as shown in Figure 7. Then above equation was applied to the available AIMP volume and a pseudo-porosity volume had been obtained.

2. The inversion-derived pseudo-porosity was compared with the CPI porosity at well X that showed peak values above 0.2 (20% porosity) (Figure 8), an evident population around 0.15, and an average porosity of the reservoir layer around 0.12, as shown by the histogram in Figure 9. As expected, the pseudo-porosity obtained from inversion provides us a result with a frequency content similar to the seismic data. For this reason the calculated porosity is not able to describe the internal porosity variations of the G-sand but is capable to catch the bulk character of the target sand (Figure 10). In detail, we can observe that the maximum value that can be attained by the pseudo-porosity inside the G-sand reservoir at X well location is 12%. It corresponds to the average porosity calculated for the same interval on CPI logs (Figure 10). According to this calibration, the pseudo-porosity away from the well site must be interpreted as indicative of the average porosity of the reservoir layer.
3. The map of the predicted average porosity in the G-sand was generated by extracting the maximum amplitude on the pseudo porosity volume from a window covering the G-sands. On the basis of this map a new well Y with a porosity prediction of 17-18% was located.

WELL Y WIRELINE LOGS AND PETROPHYSICAL ANALYSIS

The well 'Y' was a successful well, and tested gas at a rate of 15mmscfd. The porosity in well 'Y' came close to the predicted value of 17-18 %. In this well open hole wire-line logs were recorded over the G-sand interval (3283-3326m) in the final 6 inch hole, the logging suite and the depth intervals are mentioned in Table 1. The hole condition generally seems good, with only one rogues section of the hole from 3362 to 3415 m MD. Several smooth washouts are present in the G-sand interval, but their effect on the logs seems to be negligible. The caliper shows 17m of good hole (3296-3313m) while the rest enlarged up to 9-10 inch as shown in Figure 14.

The ECS (Elemental Capture Spectroscopy) logging was performed from 3115m to 3489m. The main objective of the ECS logging was to resolve the complex mineralogy associated with the Lower Goru sand units, especially the G-sand unit, which contain excessive amount of Chamosite and Glauconite.

Porosity evaluation from sonic and core data
Table 1

Tools combination	Depth interval (m MD)
DLL-MSFL-NGS-SP	3489 – 3115
DSI-ECS-GR	3489 – 3115
LDL-CNT-GR	3505 – 3115
MDT-GR	3506 – 3511

The thickness weighted average sonic log porosity of 17.5 % was calculated over the gross 43m G-sand interval

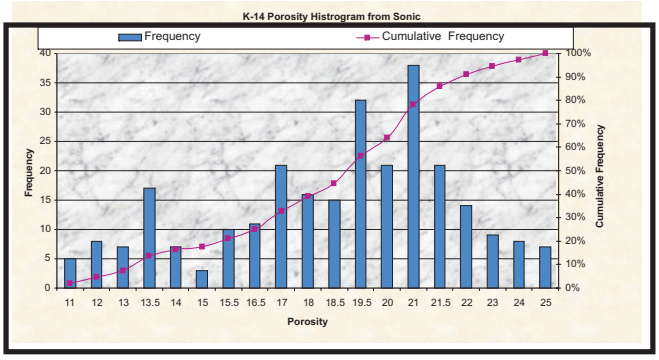

Figure 11- Well Porosity Histogram from sonic

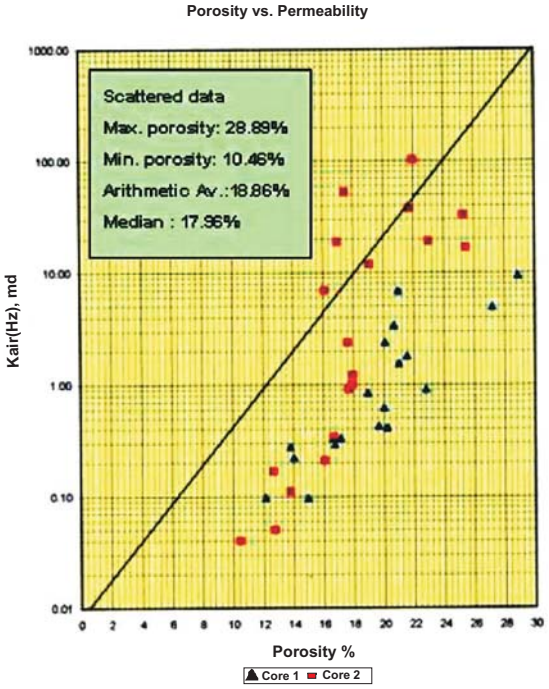

Figure 12- Well Y Routine Core Studies

(3283m-3326m) Figure 14. However, the sonic log porosity histogram shows varying porosity distributions and gives most likely occurrence of 18.7% porosity (Figure 11). The routine core analysis also showed scattered porosity data (in line with the sonic log porosity), ranging from 10.5 to 29.0 % porosity as shown in Figures 12 and 13. The arithmetic average of 18.86% porosity was as calculated with the median value of 17.96%.

Petrophysical analysis

The average porosity from sonic log and routine core analysis was very similar. However, the porosities derived from ELAN Plus, a probabilistic computer application, which calculates mineral and fluid volumes by solving a set of simultaneous equations, were quite low ranging from 6.0-17.0% as shown in Figure 15. The ELAN interpretation was

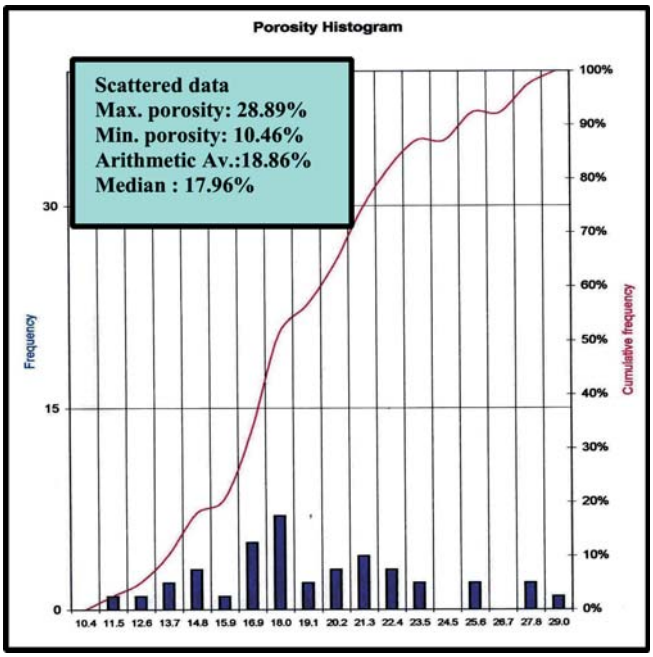

Figure 13- Porosity Histogram of Well Y from Core Data

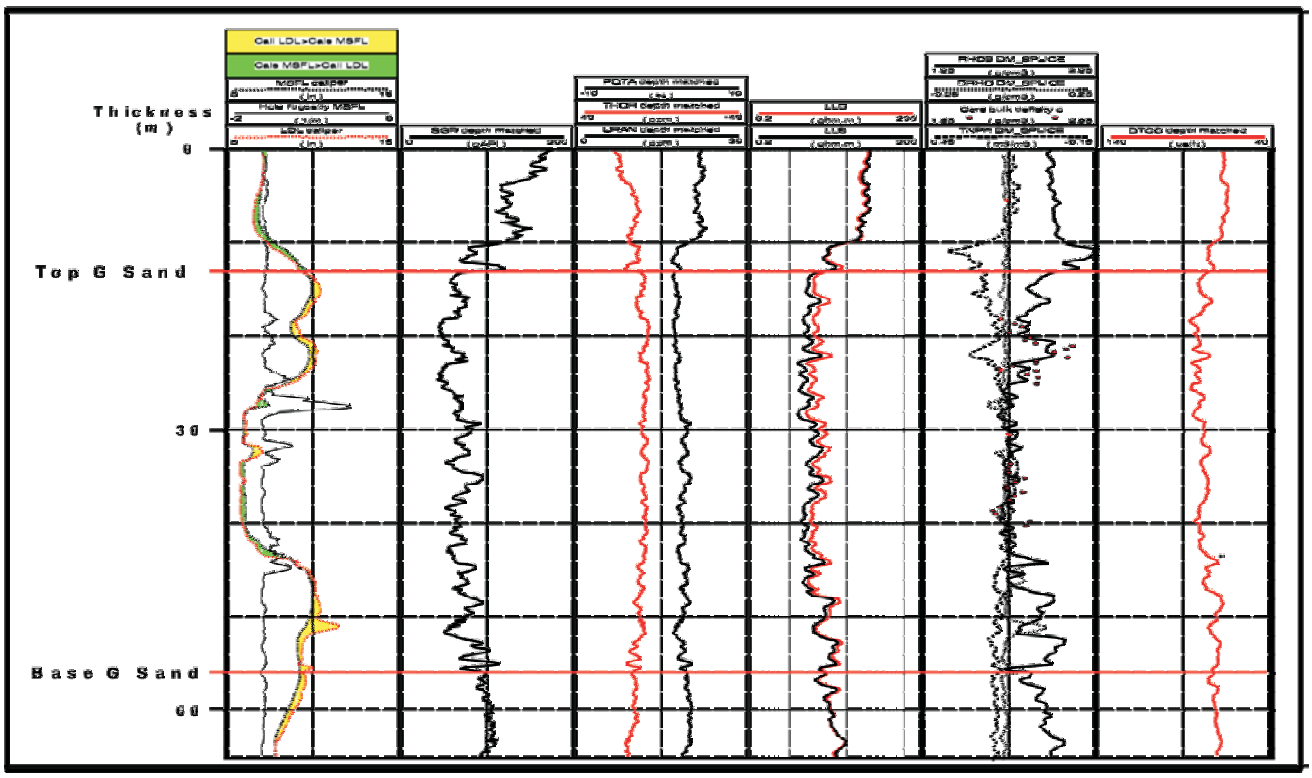

Figure 14- 'Y' Well Log over G sand Interval

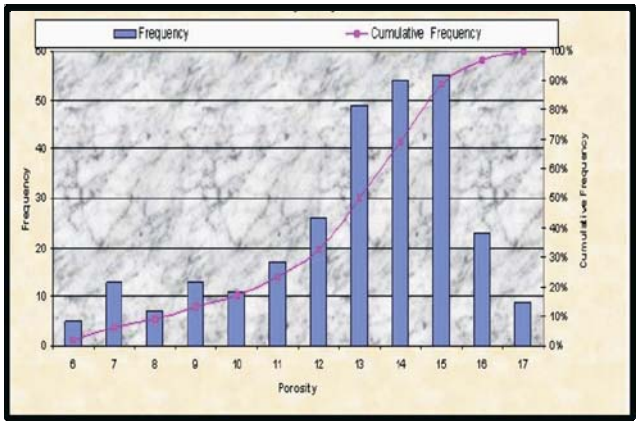

Figure 15- 'Y' Well Porosity Histogram from CPI

carried out using the Dual Water Model, and the interpretation parameters used are the same as the other adjacent wells (Figure 14). The difference between the sonic, core porosity and the porosity calculated from the ELAN can be due to several factors, among which log interpretation model uncertainty is the one. The presence of Chamosite and Fe-chlorite adversely affects the interpretation. Chlorite is a group of minerals with highly variable composition and density (from less than 2.5 to more than 4 according to the elements in the lattice, and 3.2 for Chamosite); when high volumes are calculated (like in Kadanwari wells) a small change in the assumed density can have a considerable impact on the calculated porosity, and since their composition is variable, the uncertainty remains high. To resolve the complex mineralogy, ECS logging was conducted over the entire G-sand unit. The preliminary results of ECS processing were inconclusive because the existing mineral models used in the SpectroLith processing considered only siderite for iron-rich minerals and this was not valid for this environment which contain Chamosite and Glauconite. Therefore, the accuracy of the computed mineral weight percents was questionable. To further resolve the associated mineralogy, the ECS data is under further evaluation.

CONCLUSION

The porosity prediction at well Y location was very successful. After the success of well Y which was a result of successful application of the porosity prediction method explained above, the partners of Kadanwari gas field decided to acquire 3D seismic over the remaining part of the field to use the same technology to locate good porosity zones . We consider that this method has a wide application in the Middle Indus Basin of Pakistan, but proper amplitude preservation of seismic data is a key to success.

REFERENCES

Debeye, H.W.J. and P. Van Riel,1990, Lp-Norm Deconvolution, Geophys. Prosp. 38, p. 381.

Nasir Ahmad, Arshad H. Palekar, Jawad Ahmed, Masking of Commercially Viable Reservoir intervals by Complex Mineralogy; F-sand Gas Reservoir in Kadanwari Field Pakistan. PAPG- SPE Proceedings of Annual Technical Conference, held on 2002.

Nasir Ahmed and Siddique Chaudhry, 2002, Kadanwari Gas Field, Pakistan: A disappointment turns into an attractive development opportunity, Petroleum Geoscience, v. 8, 2002, p. 307-316.

Pendrel, J.V. and P. Van Riel, 1997, Methodology for seismic inversion A Western Canada Reef Example, CSEG Recorder 22, no. 5, P.%

PJHR

Received Feb. 1, 2007, revised May 5, 2008 and accepted October 28, 2008. First the paper was presented in Annual Technical Conference of PAPG - SPE held in Islamabad, Pakistan, Oct. 08-09, 2004 and published in its proceedings. Now the paper is being published after subjecting it to refereeing process outlined by Higher Education Commission , Islamabad, Pakistan.